

# UCSF

## UC San Francisco Previously Published Works

### Title

Large-Scale Analysis of Meniscus Morphology as Risk Factor for Knee Osteoarthritis.

### Permalink

<https://escholarship.org/uc/item/54g2p6f8>

### Journal

Arthritis & Rheumatology, 75(11)

### Authors

Gao, Kenneth

Xie, Emily

Chen, Vincent

et al.

### Publication Date

2023-11-01

### DOI

10.1002/art.42623

Peer reviewed



Published in final edited form as:

*Arthritis Rheumatol.* 2023 November ; 75(11): 1958–1968. doi:10.1002/art.42623.

## Large-Scale Analysis of Meniscus Morphology as Risk Factor for Knee Osteoarthritis

Kenneth T. Gao, BS<sup>1,2</sup>, Emily Xie<sup>1</sup>, Vincent Chen, BA<sup>1</sup>, Claudia Iriondo, PhD<sup>1,2</sup>, Francesco Calivà, PhD<sup>1</sup>, Richard B. Souza, PhD<sup>1,3</sup>, Sharmila Majumdar, PhD<sup>1</sup>, Valentina Pedoia, PhD<sup>1</sup>

<sup>1</sup>Center for Intelligent Imaging, Department of Radiology and Biomedical Imaging, University of California, San Francisco, San Francisco, CA

<sup>2</sup>University of California Berkeley–University of California San Francisco Graduate Program in Bioengineering, San Francisco, CA

<sup>3</sup>Department of Physical Therapy and Rehabilitation Science, University of California, San Francisco, San Francisco, CA

### Abstract

**Objective:** While it is established that structural damage of the meniscus is linked to knee osteoarthritis (OA) progression, the predisposition to future development of OA due to geometric meniscal shapes is plausible and unexplored. This study aims to identify common variations in meniscal shape and determine their relationships to tissue morphology, OA onset, and longitudinal changes in cartilage thickness.

**Methods:** 4,790 participants from the Osteoarthritis Initiative dataset were studied. A statistical shape model was developed for the meniscus and shape scores were evaluated between a control group and an OA incidence group. Shape features were then associated with cartilage thickness changes over 8 years to localize the relationship between meniscus shape and cartilage degeneration.

**Results:** Seven shape features between the medial and lateral menisci were identified to be different between knees that remain normal and those that develop OA. These include length-width ratios, horn lengths, root attachment angles, and concavity. These “at-risk” shapes were linked to unique cartilage thickness changes that suggest a relationship between meniscus geometry and decreased tibial coverage and rotational imbalances. Additionally, strong associations were found between meniscal shape and demographic subpopulations, future tibial extrusion, and meniscal and ligamentous tears.

**Conclusion:** This automatic method expanded upon known meniscus characteristics that are associated with the onset of OA and also discovered novel shape features that have yet to be investigated in the context of OA risk.

---

**Corresponding Author:** Name: Kenneth T. Gao, Address: 1700 4th Street - 203D Byers Hall, San Francisco, CA 94158, Telephone: (415) 549-6136, Fax: (415) 353-9656, kenneth.gao@ucsf.edu.

The authors have no conflicts of interest with respect to the contents of this study.

## INTRODUCTION

One of the leading causes of global disability [1], knee osteoarthritis (OA) is a whole joint disease with complex, multifactorial pathophysiology [2]. The growing recognition of interactions between structural tissues of the knee joint have pushed the research community to categorize distinct OA phenotypes using biochemical and imaging findings [3]. Traditionally, articular cartilage degeneration and changes in subchondral bone have been established as the foremost biomarkers of disease; however, the meniscus has garnered attention for its integral role in dispersion of load to the articular cartilage and overall mechanical stability of the joint [4,5]. Damage to the meniscus, particularly tears and extrusion from the tibial plateau, are strongly associated with knee pain, cartilage loss, and OA progression [6–11]. Several widely disseminated semiquantitative imaging scoring systems have acknowledged meniscal injury as one of the main structural phenotypes in the standardized assessment of knee OA [12–14].

While links between meniscus injury and knee OA are well established, the characterization of the geometric shape of the meniscus and its relationship with knee OA remains a challenging area of research. Past efforts identify and manually measure meniscal shape features hypothesized to be associated with OA risk factors. Wirth, *et al.* [15], segmented the meniscus from 31 proton density-weighted magnetic resonance images (MRIs) of knees with and without radiographic OA and found that knees with OA had greater meniscus volume, surface area, thickness, and increased extrusion. Kawahara, *et al.* [16], similarly extracted measurements from menisci of 51 subjects using manual segmentation of T<sub>1ρ</sub>-weighted MRI. Knees in the severe OA group were characterized with larger longitudinal diameter and posterior wedge angle and smaller posterior wedge width of the medial meniscus. Recently, Wenger, *et al.* [17], discovered that both the medial and lateral menisci of OA knees bulged at the periphery and were more extruded, and additionally, the lateral menisci were larger in volume. Exploration of meniscus geometry has uncovered aspects of the relationship between coverage, disruption of cartilage, and OA but may be insensitive to nuanced shape features beyond the engineered constructs specified in the abovementioned studies. Moreover, due to the complexity of meniscus morphologies, there is a need to evaluate shape on a much larger scale.

The recent surge of deep learning-based segmentation techniques has impacted various areas of imaging-derived morphological analyses, including those of knee OA. The U-Net [18] and other convolutional neural network models have been shown to delineate cartilage, bone, meniscus, and other soft tissues with high reproducibility, equivalent to or surpassing human inter-operator variability [19–25]. Specialized techniques have pushed the performance of knee joint segmentation models, including anatomical shape-assisted model training [19], self-attention mechanisms [20], and adversarial learning schemes [22]. Irrespective of the underlying components, deep learning-based models have quickly become pervasive for their ability to automatically output high-quality segmentation of complex structures.

The capacity to expeditiously extract and analyze tissue morphology with deep learning has enabled advancements in large-scale shape analysis. Benefitting greatly from increased sample sizes, statistical shape modeling (SSM) is a technique that parameterizes and

compactly describes population-level geometric features [26]. The methodology, grounded in computer vision, commonly begins by algorithmically matching anatomical landmarks between subjects. By forming this inter-subject correspondence, the geometric variations within a population can be quantified and then condensed into a hierarchy of major modes of deviation from the average shape. A key advantage to SSM is the aspect of statistical parameterization, which allows for the identification and reconstruction of tissue geometries representative of subpopulations. Several shape models have been developed for the knee joint to describe variations in bone shape such as intercondylar narrowing in subjects with acute anterior cruciate ligament injuries [27], prominence of the medial tibial spine in athletes with high-knee impact [28], and classical structural signs of disease progression in OA patients [29–31]. Notably, Bowes, *et al.* [31], established a quantitative SSM measure of bone shape to reflect OA status, a step towards the development of personalized shape metrics. While limited by small sample sizes, pilot shape models have been developed for the meniscus as well [32,33], typically utilizing manual or semiautomatic techniques. Automated shape extraction and data-driven analysis powered by expanded sample sizes capable of capturing natural shape variability would greatly benefit the discovery of the relationships between meniscal morphology and OA onset or progression.

In this study, we leveraged deep learning-based segmentation of multiple tissues in the knee joint to perform shape analysis of the meniscus. We constructed an SSM of the meniscus with the following aims: (1) to identify meniscus shapes associated with future onset of OA, and (2) to localize future changes in cartilage thickness with respect to at-risk meniscus shapes. This automated methodology was scaled for evaluation of the Osteoarthritis Initiative (OAI), a multicenter, prospective, observational imaging dataset sponsored by the National Institutes of Health.

## PATIENTS AND METHODS

This analysis utilized baseline MRI acquisitions from the OAI dataset to generate a statistical model of meniscus shape. Shape features associated with future development of OA were identified via group analysis between a healthy *Control* group and an *OA Incidence* group. Each baseline meniscus shape was subsequently evaluated with longitudinal cartilage thickness changes. The study design overview is outlined in Fig. 1A.

### Dataset

Imaging data was obtained from the 4,796 participants with, or at risk for, symptomatic femoral-tibial knee OA enrolled in the OAI study. Knee radiographs and MRIs (Siemens Trio 3.0 Tesla) were acquired annually at baseline to 48-month visits, and every two years between 48-month and 96-month visits [34,35].

Kellgren-Lawrence (KL) grades of OA severity were performed centrally using bilateral PA fixed flexion knee radiographs to describe cases with osteoarthritic signs of cartilage and bone such as joint space narrowing and osteophytes. Meanwhile, MRIs were graded with the MRI Osteoarthritis Knee Score (MOAKS) system by the Boston Imaging Core Lab, encapsulating morphological and signal abnormalities of the cartilage, bone, meniscus, ligaments, and tendons.

9,418 knee MRIs at the baseline timepoint from 4,790 participants were used to build the meniscus shape model. Six participants were excluded due to unavailable imaging. Statistical analysis considered 5,009 knees from 3,103 participants with no OA (KL grade 1) at baseline. In the longitudinal cartilage thickness analysis, 1,419 knees from the 1,036 participants with complete MRIs at all seven timepoints were included. Demographic data of all participants and the abovementioned subsets can be found in Supplementary Table S1.

## Image Processing

The summary of the technical methodology is illustrated in Fig. 1B.

**Tissue Segmentation**—With high spatial resolution and excellent delineation of the cartilage-bone and cartilage-meniscus interfaces [35], sagittal 3D dual-echo steady-state images with selective water excitation (DESS-we) were automatically segmented to extract tissue morphology. This was performed using neural network-based models that have been trained and validated for the OAI in previous efforts [36,37]. Performance of these models were measured using mean (standard deviation [SD]) Dice coefficients to describe average overlap between human-annotated and model-predicted segmentations: meniscus = 0.874 ( $\pm 0.024$ ), femur = 0.972 ( $\pm 0.011$ ), tibia = 0.973 ( $\pm 0.013$ ), femoral cartilage = 0.890 ( $\pm 0.023$ ), and tibial cartilage = 0.880 ( $\pm 0.036$ ). Additional information regarding model training, performance, and validation can be found in Supplementary Section A.

**Automatic Landmark Correspondence**—Next, the segmentation masks of the meniscus and bones were transformed to triangular meshes using the Marching Cubes algorithm [38]. This effectively reduced the complexity of tissue morphology to its surface topology.

A healthy knee within the dataset was chosen to serve as an atlas. The criteria for atlas selection were as follows: (1) KL grade = 0, (2) no meniscal abnormalities by MOAKS, (3) no imaging abnormalities, and (4) minimal deviation from mean age and BMI of the dataset. After flipping knees of opposite laterality (i.e., right versus left) to match the atlas, all surface meshes were then algorithmically aligned. For the menisci, this included scaling to the size of the atlas menisci, rigid alignment using Iterative Closest Point, and re-scaling to the original size. Due to the prominence of anatomical bony features, the femur and tibia were instead independently aligned using a landmark matching algorithm [39]. With the atlas-matched correspondence, geometric features of the surface topology could be compared in the downstream statistical analysis. The mesh processing pipeline is reported in full detail in Supplementary Section B.

**Statistical Shape Modeling of the Meniscus**—Principal component analysis (PCA) of the matched meniscal meshes served to reduce the dimensionality of the feature-spaces from  $n_m$  and  $n_l$  to  $k$ , where  $n_m$  and  $n_l$  are the numbers of x, y, and z coordinates of the vertices in the medial and lateral menisci surface meshes, and  $k$  is a designated number of representative shape features, known as modes of variation [27]. To highlight shapes as risk factors for OA, only meshes of baseline visits were considered to build the initial  $n_m$

and  $n_T$ -dimensional spaces. Each mode was then assessed by simulating variation around the mean shape to assign a morphological description to the quantitative variance.

**Localization of Cartilage Thickness Trajectories**—Cartilage thickness values were encoded to the subchondral surfaces of the bone mesh. Thicknesses were derived using a Euclidean distance transform of the binary cartilage segmentation mask on a slice-wise basis. The distance maps were skeletonized along the long axis of each cartilage and encoded to the nearest vertex of the surface mesh.

Longitudinal changes in cartilage thickness, i.e., thickness velocities, were computed for participants with complete MRI across the seven timepoints (baseline to 8 years). Velocities at each vertex of the cartilage skeletons were independently computed as the first-order derivatives of the observed thicknesses and averaged to estimate future localized thinning or thickening from baseline.

### Statistical Analysis

To determine meniscus shape features associated with future OA incidence, two groups were established: (a) *Control*: knees with KL grade of 0 or 1 throughout participation in the OAI, and (b) *OA Incidence*: knees with KL grade of 0 or 1 at baseline and subsequent incidence of radiographic OA (KL grade  $\geq 2$ ) within 8 years. Group analysis was performed using one-way analysis of covariance and least-squares mean, controlling for age, sex, race, and body mass index (BMI). Statistical significance was established as  $p < \frac{0.05}{k}$  to correct for independent comparisons of each mode.

It is plausible that meniscal damage, such as tears and extrusion, are linked with meniscal shapes identified as OA risk factors. To investigate this assumption, knees in the *Control* and *OA Incidence* groups with complete MOAKS grading for meniscal anterior, body, and posterior tears, posterior root tear, and anterior extrusion were fitted in a multiple linear regression using at-risk meniscal shapes, the aforementioned MOAKS grades, and demographics (age, sex, race, and BMI) as predictors for OA incidence.

Additional analysis was performed to establish cross-sectional patterns in meniscus shapes with relevant demographic subpopulations. One-way analysis of covariance was used to evaluate differences in gender, while Pearson correlation assessed associations with age, height, weight, and BMI. Demographic values were extracted from the baseline visit.

Furthermore, the prognostic capacity of meniscus shapes and their relationship to future development of common imaging abnormalities were assessed. These included tears of the anterior horn, meniscal body, posterior horn, posterior root, and anterior cruciate ligament (ACL), as well as extrusion from the tibial plateau. Similar to the evaluation of OA incidence, subgroups were delineated as subjects that remained healthy and those that developed meniscal injuries within four years, as determined by MOAKS grading. Damage to the posterior cruciate ligament was not considered due to insufficient number of grades.

To establish relationships between meniscus shape and future cartilage thickness trajectory, knees were repartitioned by PC score to either *Control-Associated Quartiles* or *OA*

*Incidence-Associated Quartiles* for each statistically significant mode. Group analysis was similarly performed to compare average velocity between quartiles.

## RESULTS

### Statistical Shape Modeling of the Meniscus

The primary ten modes of each meniscus are described in Fig. 2 and capture 90.17% and 87.71% of the total variance in the medial and lateral meniscus, respectively. More information regarding the compactness and cumulative geometric variance retained by these models can be found in Supplementary Section C.

**Demographic Analysis of Meniscus Shape**—The association matrix, in Fig. 3A, demonstrates cross-sectional relationships between meniscus shapes and demographics. Gender was the most prevalent category, with group differences between male and female in 17 of the observed 20 modes. The first mode, meniscal volume, was associated with all studied variables. Notably, shapes of the lateral meniscus were found to be more closely related to demographics than those of the medial meniscus.

**Shape-Associated Development of Meniscal Damage**—Fig. 3B describes associations of meniscus shapes with future incidence of morphological damage. In the medial meniscus, posterior root tears and medial-side extrusion were the most predictable from shape information, with statistical dependence found in 8 and 7 out of 10 modes, respectively. Other relationships with meniscal tears, ACL tears, and anterior-side extrusion were less extensive. Patterns in the lateral meniscus were, again, more prevalent than in the medial meniscus. Mode 1, volume, was found to be associated with almost all forms of future damage.

**Meniscus Shapes as Risk Factor for Future OA**—The *Control* group consisted of 2,778 subjects (1,536 female, age =  $60.2 \pm 9.2$ , BMI =  $27.6 \pm 4.5$  kg/m<sup>2</sup>) while the *OA Incidence* group contained 528 subjects (350 female, age =  $60.4 \pm 8.7$ , BMI =  $29.1 \pm 4.6$  kg/m<sup>2</sup>). Four of ten modes that describe medial meniscus shape and three of ten modes that describe lateral meniscus shape were significantly different between the *Control* and *OA Incidence* groups (Fig. 4). Features of the medial meniscus that characterized the *OA Incidence* group were described as wider transverse diameter (mode  $2_m$ ;  $p < 0.001$ ; % variance = 5.05%), longer anterior root accompanied by shorter posterior root (mode  $5_m$ ;  $p < 0.001$ ; % variance = 1.45%), flaring of the outer wall (mode  $7_m$ ;  $p < 0.001$ ; % variance = 0.87%), and increased concavity of the posterior horn and inward angling of the posterior root (mode  $8_m$ ;  $p < 0.001$ ; % variance = 0.70%). While for the lateral meniscus, we observed the following in the *OA Incidence* group: larger transverse length-width ratio (mode  $2_l$ ;  $p < 0.001$ ; % variance = 14.60%), inward angling (mode  $3_l$ ;  $p < 0.001$ ; % variance = 8.60%) and increased length of the anterior horn (mode  $5_l$ ;  $p < 0.001$ ; % variance = 1.31%).

Further investigation of the abovementioned shapes in conjunction with MOAKS grading of meniscal damage is detailed in Table 1. 703 participants from the *Control* group and 372 participants from the *OA Incidence* group were previously graded for MOAKS scoring of meniscal anterior, body, and posterior tears, posterior root tear, and anterior extrusion and



included in this analysis. The effect size of each variable is described by the regression slope coefficient. To give physical meaning to the shape variable coefficients, the slopes are scaled by one SD, i.e. one-third of the deviation illustrated in Fig. 4. In the medial meniscus, the addition of meniscal damage to the regression did not change the statistical relationship of the shape variables. The coefficients of all four modes increased, indicating higher response to OA incidence after adjusting for tears and extrusion. Of the MOAKS variables, posterior tears and anterior extrusion were expectedly statistically associated with OA incidence. The effect size of these forms of damage are equal to approximately 3 SD of the shape variables. In the lateral meniscus, anterior extrusions were associated with OA incidence, accounting for five times the average response of mode  $3_l$ . Modes  $2_l$  and  $5_l$  were no longer statistically significant with the inclusion of meniscal damage variables.

### Meniscus Shape-Associated Cartilage Thickness Trajectories

In the femur, knees of both the *Control* and *OA Incidence* groups were observed with overall cartilage thinning when spatially averaged: mean (SD) rate of  $-0.0026 (\pm 0.0038)$  mm/year and  $-0.0035 (\pm 0.0057)$  mm/year, respectively. 54.1% ( $\pm 10.0\%$ ) of the cartilage surfaces in the *Control* velocity maps demonstrated thinning, as compared to 53.0% ( $\pm 12.4\%$ ) of the surfaces in the *OA Incidence* maps. Similar patterns were seen in the tibial cartilage trajectories. Average velocities were  $-0.0044 (\pm 0.0057)$  mm/year and  $-0.0067 (\pm 0.0073)$  mm/year with thinning in 62.2% (12.0%) and 64.8% (12.3%) of the surfaces in the *Control* and *OA Incidence* groups, respectively.

Localized associations between meniscus shape and cartilage trajectory are shown in Fig. 5. In all but one assessment (mode  $8_m$ ), the velocity difference maps were predominantly negative, implying lower overall velocities (i.e., more rapid thinning or less rapid thickening) in the statistically significant regions of the *OA Incidence-Associated Quartiles* relative to those in the *Control-Associated Quartiles*. In general, regions of statistical difference in the femoral cartilage were more focal, whereas differences in the tibial cartilage were sparse and generally located around the cartilage periphery.

## DISCUSSION

In this study, we investigated the association of meniscus shape with future incidence of OA. Deep learning has enabled large-scale multi-tissue morphological evaluations. Combined with statistical shape modeling, an exploratory technique for parameterizing population-level shape features, human supervised feature engineering is no longer necessary to discover geometric characteristics of this nuanced tissue in relation to OA.

The characterization of meniscal geometry has been historically studied in the context of meniscus transplant. Several efforts have investigated non-invasive techniques for the optimization of meniscal replacement matching [40,41], such as using demographic information as predictors for meniscus size. Modes  $1_m$  and  $1_l$  in this study, representative of meniscal volume, were found to have strong relationships with gender, age, height, weight, and BMI, relating well to past work [15,17]. Our results describe gender as the most predictive of these demographics, which is consistent with a multivariate regression model developed by Van Thiel, *et al.* [40], that utilized similar variables in allograft sizing. Aside



from gender, other basic demographics were statistically correlated to several shape features; however, the strengths of correlation were relatively weak with the exceptions of height and weight to meniscus size. Notwithstanding, these results serve as a preliminary benchmark for future analyses of meniscus shape stratification in demographic subpopulations.

Overall, the SSM produced anatomically consistent shape constructs. For example, structurally, the medial meniscus has more peripheral fixation, is less mobile than the lateral meniscus [42], and often moves as a single unit [43]. This is appreciable in that variations in the medial modes were generally radial and engages multiple sections of the tissue, whereas those of the lateral meniscus were primarily found in the horns. Moreover, the medial posterior horn is the most anchored section of both menisci, and the most susceptible to damage [33]. In our results, shape variations in this area involved differences in thickness or cross-section, as opposed to length or position more commonly seen in the anterior or lateral horns. In relation to OA incidence, the shapes identified in this study are compatible with and expand upon past literature [15–17]. Features such as larger posterior wedge angle, smaller medial posterior wedge width [16], and bulging of the periphery found in OA populations [17], are related to modes identified here as OA precursors (modes  $7_m$  and  $8_m$ ). However, these relationships should be evaluated with consideration to interactions between shape and tissue damage or injury. The multivariate sub-analysis with shape and MOAKS grading in Table 1 found consistent associations with OA incidence in the medial meniscus, but two of three relationships of the lateral meniscus were no longer statistically significant, suggesting tears and extrusions playing confounding roles. It is important to note that further longitudinal analysis using this framework can help identify how meniscus shape progresses over time, both in the presence and absence of OA.

A key strength of this approach is the joint assessment of meniscal shape with future cartilage thickness changes to reveal localized patterns of knee joint degeneration. The seven shapes identified as OA risk factors each presented with unique cartilage trajectories. Group differences in the femoral compartments were more prevalent than those in the tibia, likely due to the complexity of meniscal shape being primarily in the concave meniscal-femoral interface as opposed to the flat, fixated meniscal-tibial surface.

Differences in cartilage thickness changes due to medial meniscus shapes were more prevalent than lateral meniscus shapes. Modes  $2_m$  and  $7_m$  both presented with large, central regions of increased rates of thinning in the medial femoral condyle of the *OA Incidence-Associated Quartile*, despite describing distinct shape features (wider transverse diameter and flaring of outer wall, respectively). Considering that both modes were also identified as predictors of extrusion, we suspect that these modes are linked to decreased central coverage in the medial compartment and progressive cartilage degeneration. Differences in mode  $5_m$  were more divergent, with moderately increased rates of thinning in the medial compartment and dramatically increased rates in the opposite lateral trochlea. Similarly, we observed increased thinning near the medial tibial eminence accompanied by decreased thinning in the anterolateral plateau. The meniscal shape, interpreted as an elongation of the anterior horn and perhaps influenced by the presence or prominence of the transverse ligament, may suggest rotational imbalance that causes pressure points along the medial wall of the intercondylar notch and lateral trochlea. Lastly, mode  $8_m$  also presented with

focal differences in the lateral trochlea, yet the cartilage of the *OA Incidence-Associated Quartile* thinned at a slower rate than the *Control-Associated Quartile*. This mode may be more closely related to non-cartilage subtypes or OA of the patellofemoral joint.

Relative to medial meniscus shape-related cartilage trajectories, those associated with lateral meniscus shapes were sparser. Regions of significant differences were located on both medial and lateral sides in the femoral, trochlear, and tibial compartments. Notably, medial regions tend to describe increased rates of thinning in the *OA Incidence-Associated Quartile* whereas lateral regions presented with decreased rates. This suggests that lateral meniscus shape may play a secondary role in this population with predominantly medial compartment OA.

An advantage of this approach is that it is quantitative and automated, however this also introduces some limitations. While this methodology is capable of evaluating meniscus, cartilage, and bone collectively, it lacks true localization of the overall joint structure. Secondly, discoid meniscus, an abnormal and congenital development involving morphological and structural deformations, was not evaluated in our study due to low and varied incidence rates ranging from 0.06–17% [44]. It is evident from the cartilage analysis that the trochlea, and possibly the patellar cartilage, are impacted by meniscus shape. In this work, we constrained our scope to tibiofemoral OA, yet it would be informative to evaluate patellofemoral OA in future studies.

In summary, this data-driven method presented a general foundation of common variations of meniscus geometry, broadened the description of meniscus characteristics that are associated with the onset of OA, and also discovered novel shape features that have yet to be investigated in the context of OA risk. Furthermore, localized longitudinal changes in cartilage thickness were associated with each meniscus shape, contributing additional granularity to prognosis of cartilage degeneration. This work describes a quantitative approach toward integrating meniscus morphology into the assessment of knee OA as a whole joint disease.

## Supplementary Material

Refer to Web version on PubMed Central for supplementary material.

## ACKNOWLEDGEMENTS

This work was funded by the National Institutes of Health and National Institute of Arthritis and Musculoskeletal and Skin Diseases (grant number: R00AR070902). The OAI is a public-private partnership comprised of five contracts (N01-AR-2-2258; N01-AR-2-2259; N01-AR-2-2260; N01-AR-2-2261; N01-AR-2-2262) funded by the National Institutes of Health, a branch of the Department of Health and Human Services, and conducted by the OAI Study Investigators. Private funding partners include Merck Research Laboratories; Novartis Pharmaceuticals Corporation, GlaxoSmithKline; and Pfizer, Inc. Private sector funding for the OAI is managed by the Foundation for the National Institutes of Health. This manuscript was prepared using an OAI public use data set and does not necessarily reflect the opinions or views of the OAI investigators, the NIH, or the private funding partners.

## DATA AND CODE AVAILABILITY

Tissue segmentation masks, as described by [36,37], were compiled and are available at <https://www.kaggle.com/datasets/kgao00/oai-tissue-segmentations>. The code used in this manuscript for meniscus shape modeling is available at [https://github.com/kenneth-gao/meniscus\\_ssm](https://github.com/kenneth-gao/meniscus_ssm).

## REFERENCES

1. Cross M, Smith E, Hoy D, et al. The global burden of hip and knee osteoarthritis: estimates from the Global Burden of Disease 2010 study. *Ann Rheum Dis* 2014;73:1323–30. doi:10.1136/annrheumdis-2013-204763 [PubMed: 24553908]
2. Glyn-Jones S, Palmer AJR, Agricola R, et al. Osteoarthritis. *The Lancet* 2015;386:376–87. doi:10.1016/S0140-6736(14)60802-3
3. Roemer FW, Collins J, Kwok CK, et al. MRI-based screening for structural definition of eligibility in clinical DMOAD trials: Rapid OsteoArthritis MRI Eligibility Score (ROAMES). *Osteoarthritis Cartilage* 2020;28:71–81. doi:10.1016/j.joca.2019.08.005 [PubMed: 31513920]
4. Shrive NG, O'Connor JJ, Goodfellow JW. Load-bearing in the knee joint. *Clin Orthop* 1978;;279–87. [PubMed: 657636]
5. Kurosawa H, Fukubayashi T, Nakajima H. Load-bearing mode of the knee joint: physical behavior of the knee joint with or without menisci. *Clin Orthop* 1980;;283–90.
6. Link TM, Steinbach LS, Ghosh S, et al. Osteoarthritis: MR Imaging Findings in Different Stages of Disease and Correlation with Clinical Findings. *Radiology* 2003;226:373–81. doi:10.1148/radiol.2262012190 [PubMed: 12563128]
7. Englund M, Roemer FW, Hayashi D, et al. Meniscus pathology, osteoarthritis and the treatment controversy. *Nat Rev Rheumatol* 2012;8:412–9. doi:10.1038/nrrheum.2012.69 [PubMed: 22614907]
8. Berthiaume M-J, Raynauld J-P, Martel-Pelletier J, et al. Meniscal tear and extrusion are strongly associated with progression of symptomatic knee osteoarthritis as assessed by quantitative magnetic resonance imaging. *Ann Rheum Dis* 2005;64:556–63. doi:10.1136/ard.2004.023796 [PubMed: 15374855]
9. Gale DR, Chaisson CE, Totterman SMS, et al. Meniscal subluxation: association with osteoarthritis and joint space narrowing. *Osteoarthritis Cartilage* 1999;7:526–32. doi:10.1053/joca.1999.0256 [PubMed: 10558850]
10. Englund M, Guermazi A, Roemer FW, et al. Meniscal tear in knees without surgery and the development of radiographic osteoarthritis among middle-aged and elderly persons: The Multicenter Osteoarthritis Study. *Arthritis Rheum* 2009;60:831–9. doi:10.1002/art.24383 [PubMed: 19248082]
11. Torres L, Dunlop DD, Peterfy C, et al. The relationship between specific tissue lesions and pain severity in persons with knee osteoarthritis. *Osteoarthritis Cartilage* 2006;14:1033–40. doi:10.1016/j.joca.2006.03.015 [PubMed: 16713310]
12. Kornaat PR, Ceulemans RYT, Kroon HM, et al. MRI assessment of knee osteoarthritis: Knee Osteoarthritis Scoring System (KOSS)—inter-observer and intra-observer reproducibility of a compartment-based scoring system. *Skeletal Radiol* 2005;34:95–102. doi:10.1007/s00256-004-0828-0 [PubMed: 15480649]
13. Hunter DJ, Guermazi A, Lo GH, et al. Evolution of semi-quantitative whole joint assessment of knee OA: MOAKS (MRI Osteoarthritis Knee Score). *Osteoarthritis Cartilage* 2011;19:990–1002. doi:10.1016/j.joca.2011.05.004 [PubMed: 21645627]
14. Peterfy CG, Guermazi A, Zaim S, et al. Whole-Organ Magnetic Resonance Imaging Score (WORMS) of the knee in osteoarthritis. *Osteoarthritis Cartilage* 2004;12:177–90. doi:10.1016/j.joca.2003.11.003 [PubMed: 14972335]
15. Wirth W, Frobell RB, Souza RB, et al. A three-dimensional quantitative method to measure meniscus shape, position, and signal intensity using MR images: A pilot study and preliminary

- results in knee osteoarthritis. *Magn Reson Med* 2010;63:1162–71. doi:10.1002/mrm.22380 [PubMed: 20432287]
16. Kawahara T, Sasho T, Katsuragi J, et al. Relationship between knee osteoarthritis and meniscal shape in observation of Japanese patients by using magnetic resonance imaging. *J Orthop Surg* 2017;12:97. doi:10.1186/s13018-017-0595-y
  17. Wenger A, Wirth W, Hudelmaier M, et al. Meniscus Body Position, Size, and Shape in Persons With and Persons Without Radiographic Knee Osteoarthritis: Quantitative Analyses of Knee Magnetic Resonance Images From the Osteoarthritis Initiative. *Arthritis Rheum* 2013;65:1804–11. doi:10.1002/art.37947 [PubMed: 23529645]
  18. Ronneberger O, Fischer P, Brox T. U-Net: Convolutional Networks for Biomedical Image Segmentation. *ArXiv150504597 Cs* Published Online First: 18 May 2015. <http://arxiv.org/abs/1505.04597> (accessed 14 Mar 2022).
  19. Ambellan F, Tack A, Ehlke M, et al. Automated segmentation of knee bone and cartilage combining statistical shape knowledge and convolutional neural networks: Data from the Osteoarthritis Initiative. *Med Image Anal* 2019;52:109–18. doi:10.1016/j.media.2018.11.009 [PubMed: 30529224]
  20. Byra M, Wu M, Zhang X, et al. Knee menisci segmentation and relaxometry of 3D ultrashort echo time cones MR imaging using attention U-Net with transfer learning. *Magn Reson Med* 2020;83:1109–22. doi:10.1002/mrm.27969 [PubMed: 31535731]
  21. Desai AD, Caliva F, Iriondo C, et al. The International Workshop on Osteoarthritis Imaging Knee MRI Segmentation Challenge: A Multi-Institute Evaluation and Analysis Framework on a Standardized Dataset. *Radiol Artif Intell* 2021;3:e200078. doi:10.1148/ryai.2021200078
  22. Gaj S, Yang M, Nakamura K, et al. Automated cartilage and meniscus segmentation of knee MRI with conditional generative adversarial networks. *Magn Reson Med* 2020;84:437–49. doi:10.1002/mrm.28111 [PubMed: 31793071]
  23. Norman B, Pedoia V, Majumdar S. Use of 2D U-Net Convolutional Neural Networks for Automated Cartilage and Meniscus Segmentation of Knee MR Imaging Data to Determine Relaxometry and Morphometry. *Radiology* 2018;288:177–85. doi:10.1148/radiol.2018172322 [PubMed: 29584598]
  24. Panfilov E, Tiulpin A, Nieminen MT, et al. Deep learning-based segmentation of knee MRI for fully automatic subregional morphological assessment of cartilage tissues: Data from the Osteoarthritis Initiative. *J Orthop Res* 2022;40:1113–24. doi:10.1002/jor.25150 [PubMed: 34324223]
  25. Zhou Z, Zhao G, Kijowski R, et al. Deep convolutional neural network for segmentation of knee joint anatomy. *Magn Reson Med* 2018;80:2759–70. doi:10.1002/mrm.27229 [PubMed: 29774599]
  26. Ambellan F, Lamecker H, von Tycowicz C, et al. Statistical Shape Models: Understanding and Mastering Variation in Anatomy. In: Rea PM, ed. *Biomedical Visualisation: Volume 3*. Cham: : Springer International Publishing 2019. 67–84. doi:10.1007/978-3-030-19385-0\_5
  27. Pedoia V, Lansdown DA, Zaid M, et al. Three-dimensional MRI-based statistical shape model and application to a cohort of knees with acute ACL injury. *Osteoarthritis Cartilage* 2015;23:1695–703. doi:10.1016/j.joca.2015.05.027 [PubMed: 26050865]
  28. Gao KT, Pedoia V, Young KA, et al. Multiparametric MRI characterization of knee articular cartilage and subchondral bone shape in collegiate basketball players. *J Orthop Res* 2021;39:1512–22. doi:10.1002/jor.24851 [PubMed: 32910520]
  29. Wise BL, Niu J, Zhang Y, et al. Bone shape mediates the relationship between sex and incident knee osteoarthritis. *BMC Musculoskelet Disord* 2018;19:331. doi:10.1186/s12891-018-2251-z [PubMed: 30208910]
  30. Gregory JS, Barr RJ, Yoshida K, et al. Statistical shape modelling provides a responsive measure of morphological change in knee osteoarthritis over 12 months. *Rheumatology* 2020;59:2419–26. doi:10.1093/rheumatology/kez610 [PubMed: 31943121]
  31. Bowes MA, Kacena K, Alabas OA, et al. Machine-learning, MRI bone shape and important clinical outcomes in osteoarthritis: data from the Osteoarthritis Initiative. *Ann Rheum Dis* 2021;80:502–8. doi:10.1136/annrheumdis-2020-217160 [PubMed: 33188042]

32. Vrancken ACT, Crijns SPM, Ploegmakers MJM, et al. 3D geometry analysis of the medial meniscus – a statistical shape modeling approach. *J Anat* 2014;225:395–402. doi:10.1111/joa.12223 [PubMed: 25052030]
33. Dube B, Bowes MA, Kingsbury SR, et al. Where does meniscal damage progress most rapidly? An analysis using three-dimensional shape models on data from the Osteoarthritis Initiative. *Osteoarthritis Cartilage* 2018;26:62–71. doi:10.1016/j.joca.2017.10.012 [PubMed: 29054695]
34. Eckstein F, Wirth W, Nevitt MC. Recent advances in osteoarthritis imaging—the Osteoarthritis Initiative. *Nat Rev Rheumatol* 2012;8:622–30. doi:10.1038/nrrheum.2012.113 [PubMed: 22782003]
35. Peterfy CG, Schneider E, Nevitt M. The osteoarthritis initiative: report on the design rationale for the magnetic resonance imaging protocol for the knee. *Osteoarthritis Cartilage* 2008;16:1433–41. doi:10.1016/j.joca.2008.06.016 [PubMed: 18786841]
36. Morales Martinez A, Caliva F, Flament I, et al. Learning osteoarthritis imaging biomarkers from bone surface spherical encoding. *Magn Reson Med* 2020;84:2190–203. doi:10.1002/mrm.28251 [PubMed: 32243657]
37. Iriundo C, Liu F, Calivà F, et al. Towards understanding mechanistic subgroups of osteoarthritis: 8-year cartilage thickness trajectory analysis. *J Orthop Res* 2021;39:1305–17. doi:10.1002/jor.24849 [PubMed: 32897602]
38. Lorensen W, Cline H. Marching Cubes: A High Resolution 3D Surface Construction Algorithm. *ACM SIGGRAPH Comput Graph* 1987;21:163. doi:10.1145/37401.37422
39. Lombaert H, Grady L, Polimeni JR, et al. FOCUSR: Feature Oriented Correspondence Using Spectral Regularization—A Method for Precise Surface Matching. *IEEE Trans Pattern Anal Mach Intell* 2013;35:2143–60. doi:10.1109/TPAMI.2012.276 [PubMed: 23868776]
40. Van Thiel GS, Verma N, Yanke A, et al. Meniscal Allograft Size Can Be Predicted by Height, Weight, and Gender. *Arthrosc J Arthrosc Relat Surg* 2009;25:722–7. doi:10.1016/j.arthro.2009.01.004
41. Bloecker K, Englund M, Wirth W, et al. Revision 1 Size and position of the healthy meniscus, and its Correlation with sex, height, weight, and bone area- a cross-sectional study. *BMC Musculoskelet Disord* 2011;12:248. doi:10.1186/1471-2474-12-248 [PubMed: 22035074]
42. Brantigan OC, Voshell AF. THE MECHANICS OF THE LIGAMENTS AND MENISCI OF THE KNEE JOINT. *JBSJ* 1941;23:44–66.
43. Thompson WO, Thaete FL, Fu FH, et al. Tibial meniscal dynamics using three-dimensional reconstruction of magnetic resonance images. *Am J Sports Med* 1991;19:210–6. doi:10.1177/036354659101900302 [PubMed: 1867329]
44. Yaniv M, Blumberg N. The discoid meniscus. *J Child Orthop* 2007;1:89–96. doi:10.1007/s11832-007-0029-1 [PubMed: 19308479]

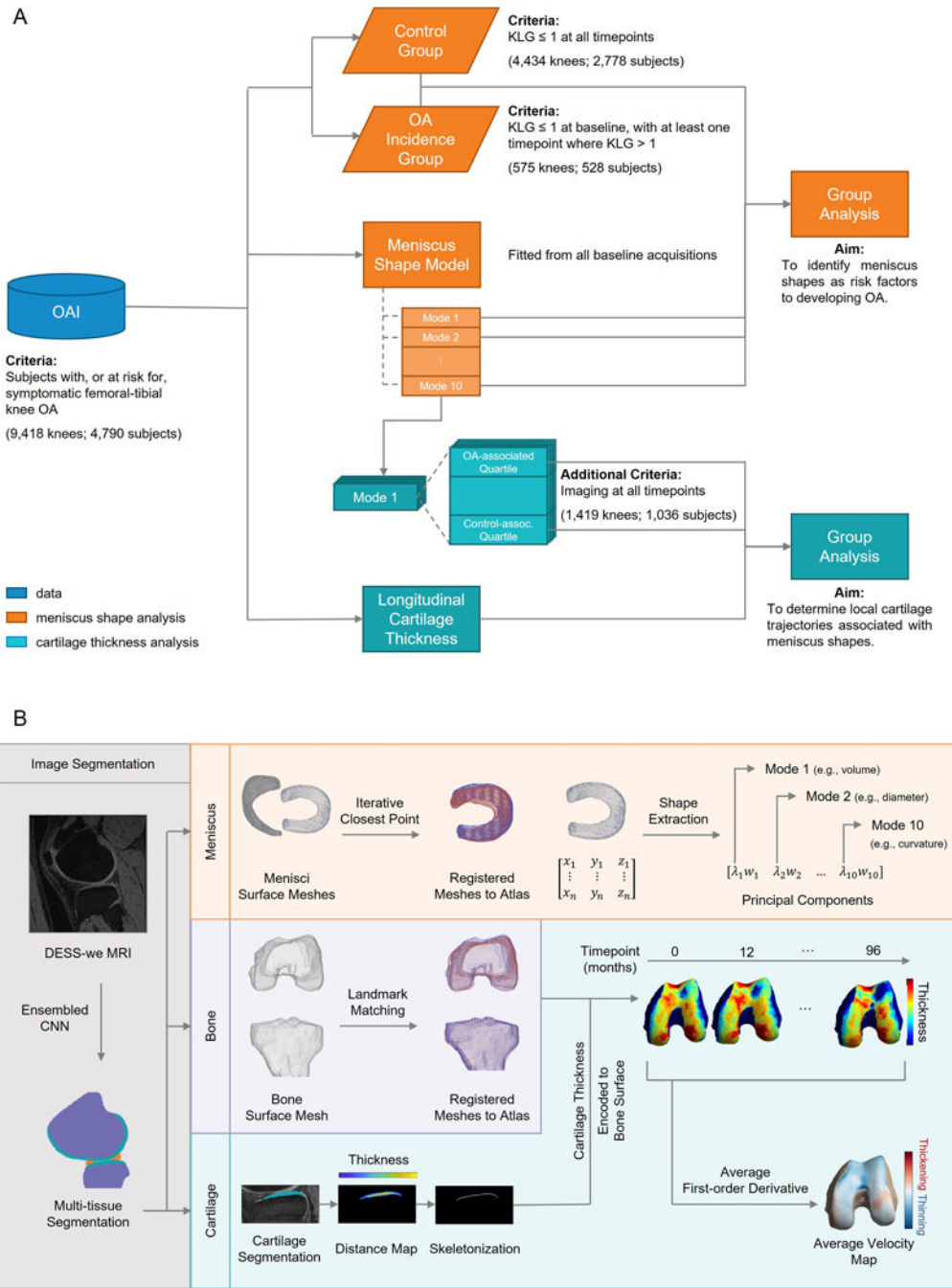


**Fig. 1.** (A) Study design. This analysis of meniscus shape utilized 4,790 DESS-we MRI acquisitions from the OAI dataset. A statistical shape model was generated for the meniscus and shape scores between the *Control* and *OA Incidence* groups identified features associated with future OA onset. These features were then assessed with localized cartilage thickness changes to investigate the link between meniscus shapes and future cartilage degeneration. (B) Schema of technical methodology. Menisci, bone, and cartilage are segmented from DESS-we MRI. The menisci are transformed into surface meshes and

registered to the menisci of a selected atlas, aligning all cases to a common coordinate system. Using PCA, geometric shape features of the meniscus can be extracted from the registered surface meshes. Meanwhile, segmentations of the femur and tibia are similarly characterized. Points on the subchondral bone are further encoded by cartilage thickness and average velocity values.

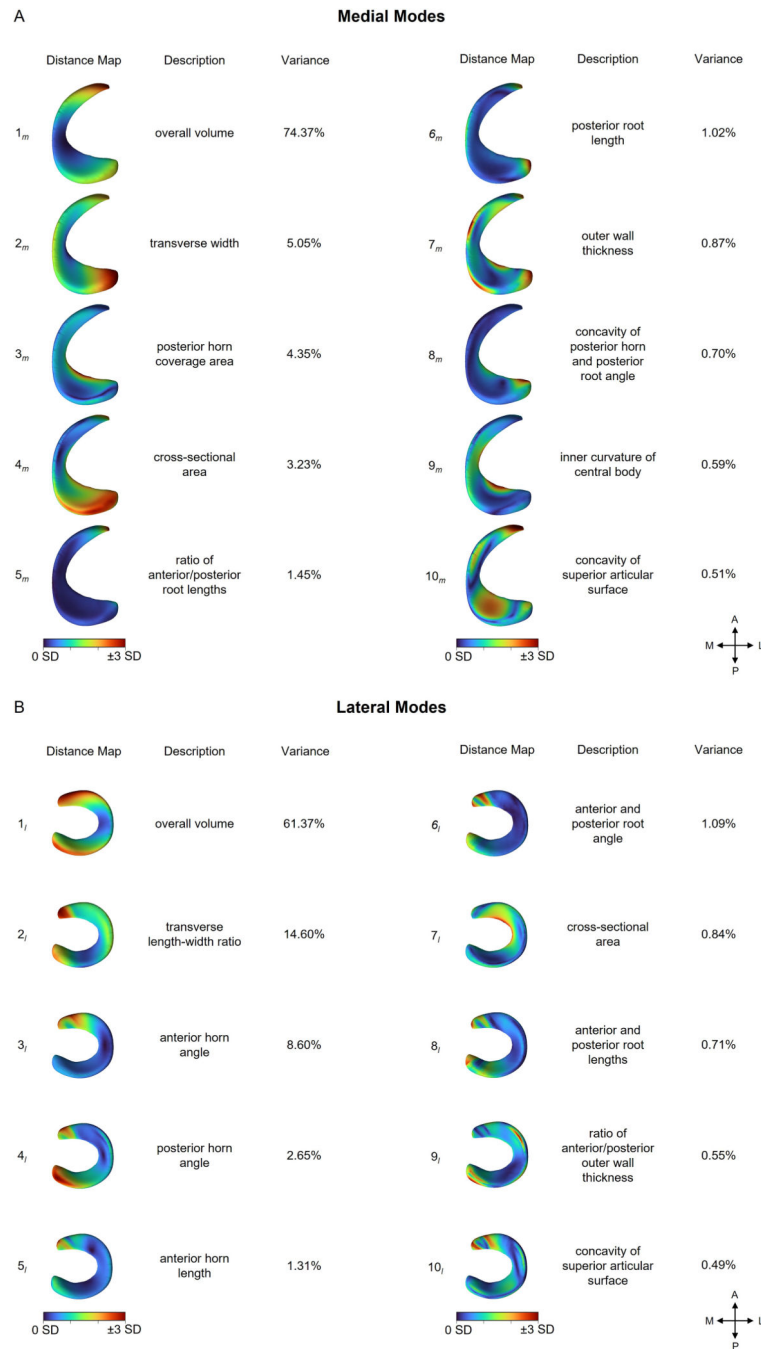
Author Manuscript

Author Manuscript

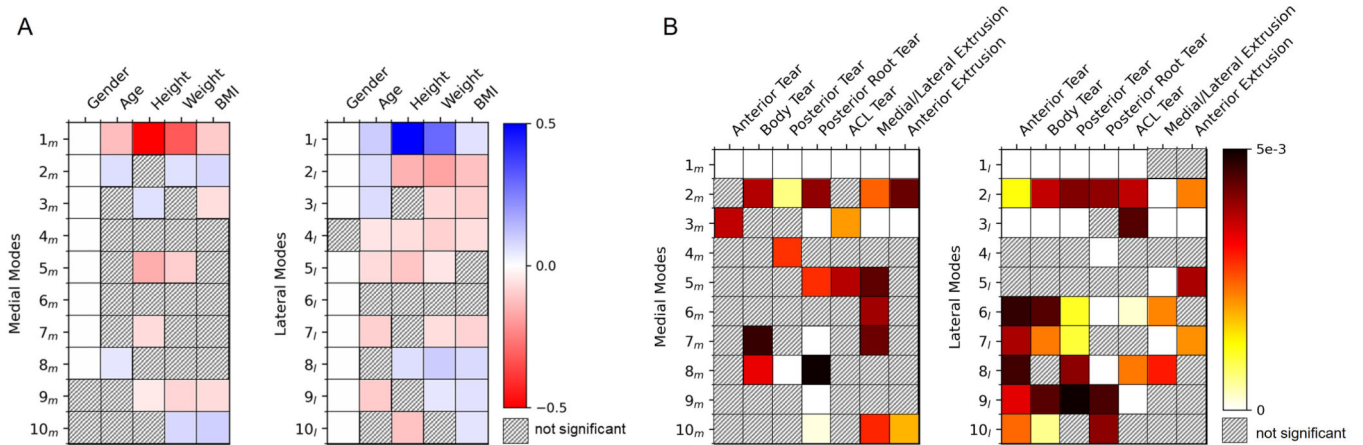
Author Manuscript

Author Manuscript





**Fig. 2.** Modes of meniscus shape produced by PCA eigendecomposition of the geometric feature covariance. The visualization depicts the renderings of the average surface with color overlay of the Euclidean norm at  $\pm 3$  standard deviations (SD). Modes are ordered by amount of variance captured by projection to each principal component.

**Fig. 3.**

(A) Demographic analysis of meniscus shapes. Statistical significance ( $p < 0.005$ ) was determined with ANCOVA for gender, and Pearson correlation for age, height, weight, and BMI. In the correlation analysis, the cell colors map to the  $R$ -value. (B) Prognostic analysis of meniscus shapes with presence of morphological imaging findings. Heatmap colors represent significant differences between menisci that develop damage within four years and those that remain normal, while grey cells depict non-statistical significance.

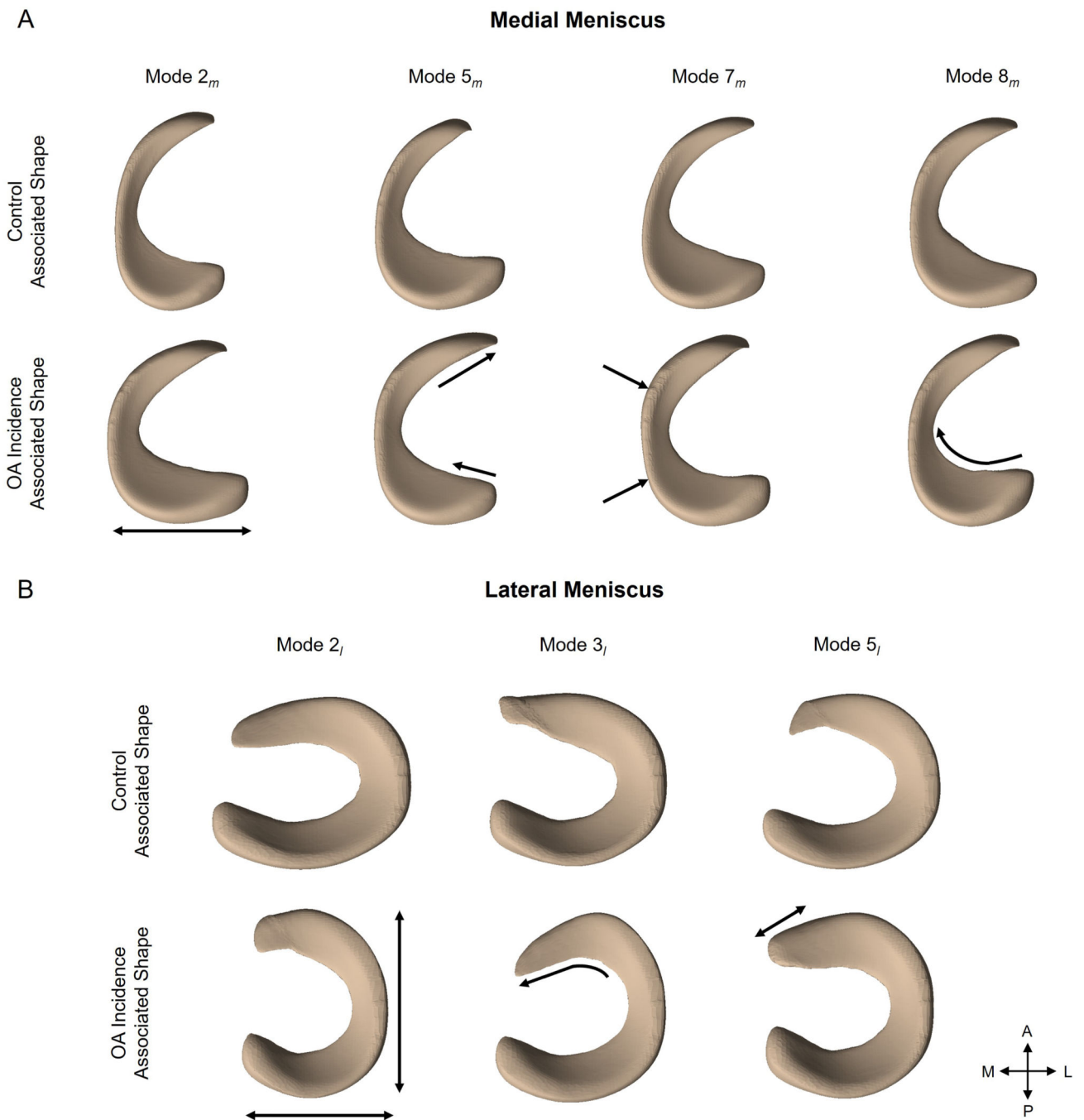


**Fig. 4.** Statistically generated (A) medial and (B) lateral menisci representative of the *Control* and *OA Incidence* groups. The modes depicted, four in the medial side and three in the lateral side, were determined to be precursors to OA incidence. Arrows depict the qualitative shape interpretation that describe the *OA Incidence* group.

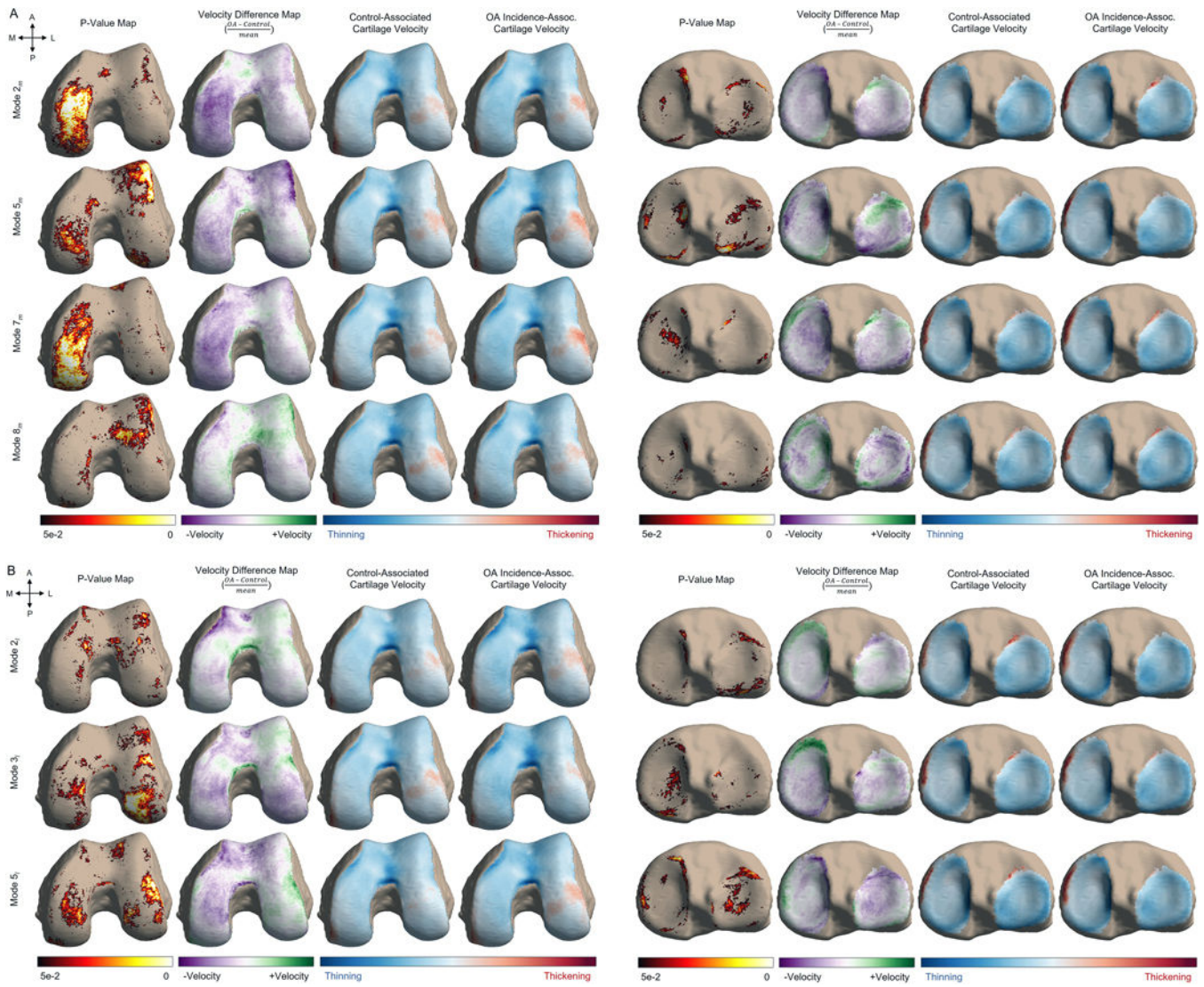


**Fig. 5.** Cartilage thickness changes within the femoral and tibial compartments in relation to (A) medial and (B) lateral meniscus shapes. The significant focal cartilage thinning of the medial condyle in modes  $2_m$  and  $7_m$  may be attributed to decreased meniscal coverage. In mode  $5_m$ , the increased length of the meniscal anterior horn may contribute to the thinning pattern in the opposite posterolateral tibia. The femoral velocity map of mode  $8_m$  is the only studied feature in which the majority of significant points demonstrated decreased rates of cartilage thinning in the *Incidence* group. Mode  $2_l$  depicts a medial-lateral imbalance in the anterior aspect of the femoral cartilage. Mode  $3_l$ , the inward angling of the meniscal anterior horn, may contribute to the significant thinning of femoral cartilage in the same area. Conversely, the increased length of the anterior horn in mode  $5_l$  is associated with cartilage thickening in the lateral femoral cartilage and thinning in the lateral tibial compartment.

**Table 1.**

Comparison of effect size and relationship of meniscal shapes and damage with OA incidence

Independent Variable	Regression Slope Coefficient <sup>c</sup>	
	Shape Only	Shape and Damage
<i>Medial Meniscus Shape</i>		
Mode 2 <sub>m</sub>	0.0148 *	0.0385 *
Mode 5 <sub>m</sub>	0.0182 **	0.0351 *
Mode 7 <sub>m</sub>	0.0259 **	0.0382 *
Mode 8 <sub>m</sub>	0.0186 **	0.0452 *
<i>Medial Meniscus Damage</i>		
Anterior Tear	--	-0.0297
Body Tear	--	-0.0914
Posterior Tear	--	0.133 *
Posterior Root Tear	--	-0.017
Anterior Extrusion	--	0.0985 *
<i>Lateral Meniscus Shape</i>		
Mode 2 <sub>l</sub>	-0.00287 *	0.00389
Mode 3 <sub>l</sub>	0.0449 *	0.0368 *
Mode 5 <sub>l</sub>	0.0299 *	0.0267
<i>Lateral Meniscus Damage</i>		
Anterior Tear	--	0.153
Body Tear	--	-0.0724
Posterior Tear	--	-0.0063
Posterior Root Tear	--	-0.353
Anterior Extrusion	--	0.182 *

\* :  $p < 0.05$ \*\* :  $p < 0.001$ <sup>c</sup> : Shape coefficients are scaled by one standard deviation